

C1

### Sodium sensitive and insensitive copper accumulation by isolated intestinal cells of rainbow trout, *Oncorhynchus mykiss*

J. Burke and R.D. Handy

School of Biological Sciences, University of Plymouth, Plymouth, UK

The pathway(s) for copper (Cu) uptake across the mucosal membrane into intestinal cells has not been elucidated, and may include Cu uptake by the Cu-specific pathway encoded by *Ctr1* or via Cu uptake through epithelial sodium channels (ENaCs). Our laboratory has developed a model of intestinal Cu absorption using a comparative physiological and genomic approach (Handy *et al.* 2000; Handy *et al.* 2002). In this study we aimed to explore whether or not Cu entry into intestinal cells was Na<sup>+</sup>-sensitive. Copper accumulation in freshly isolated intestinal cells from rainbow trout was measured by ICP-AES after exposure to 0-800  $\mu$ M CuSO<sub>4</sub> for 15 minutes. Cu accumulation by cells was  $1.88 \pm 0.52$  compared with  $0.05 \pm 0.01$  nmol Cu/mg cell protein/h with external Cu (Cu<sub>o</sub>) of 800  $\mu$ M and no-added Cu<sub>o</sub> respectively (mean  $\pm$  S.E.M., n = 6; Kruskal Wallis, P<0.05). Deduction of a rapid Cu accumulation on/in cells at time zero (about 12% of the total Cu when Cu<sub>o</sub> was 800  $\mu$ M) revealed a saturable uptake curve which reached a plateau at 400  $\mu$ M Cu<sub>o</sub> (K<sub>m</sub>, 216  $\mu$ M Cu<sub>o</sub>; V<sub>max</sub>, 1.09 nmol Cu/mg cell protein/h, 140 mM NaCl throughout). Incubating cells at 4°C did not stop Cu accumulation. Lowering external Na<sup>+</sup> to 11 mM (low Na<sub>o</sub>) generally decreased Cu accumulation into the cells over 15 min. In low Na<sub>o</sub> conditions Cu accumulation was exponential (non-saturable). Na<sup>+</sup>-insensitive Cu accumulation dominated (59% of total Cu accumulation) when Cu<sub>o</sub> was 400  $\mu$ M or less. At high Cu<sub>o</sub> (800  $\mu$ M), removal of Na<sup>+</sup> caused a 45% increase in Cu accumulation. Pre incubation of cells with epithelial Na<sup>+</sup> channel (ENaC) blocking agents for 15 minutes (normal NaCl throughout) caused Cu accumulation to increase by 40 fold (100  $\mu$ M phenamil), 21 fold (10  $\mu$ M CDPC) or 12 fold (2 mM amiloride) when Cu<sub>o</sub> was 800  $\mu$ M compared to drug-free controls (all significantly different from drug-free controls, Kruskal Wallis, P<0.05). Lowering external chloride (Cl<sub>o</sub>) from 131.6 to 6.6 mM (replaced by Na<sup>+</sup> gluconate) caused Cu accumulation to increase 11 fold when Cu<sub>o</sub> was 800  $\mu$ M. Application of 0.1 mM DIDS (normal Cl<sub>o</sub>) caused a similar effect. Lowering external pH from 7.4 to pH 5.5 produced a 17 fold, saturable, increase in Cu accumulation which was not explained by increased instantaneous Cu accumulation on/in cells at low pH. We conclude that Cu accumulation by intestinal cells is mainly Na<sup>+</sup>-insensitive and more characteristic of a *Ctr1*-like pathway than Cu uptake through ENaCs.

Handy RD *et al.* (2000) J. Exp Biol. **203**, 2365-2377.Handy, RD *et al.* (2002) Biochimica Biophysica Acta- Biomembranes. **1566**, 104-115.

This work was funded by a Leverhulme Trust grant to R. Handy.

Where applicable, the experiments described here conform with Physiological Society ethical requirements.

C2

### Piracetam and TRH Antagonise Inhibition of D-Glucose transport in human erythrocytes by Barbiturates and Diazepam

I. Afzal, R.J. Naftalin and P. Cunningham

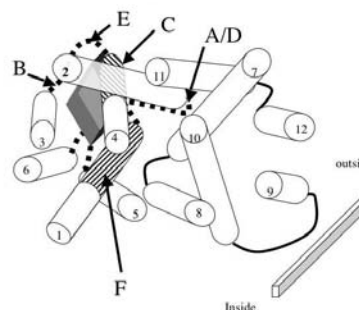
Cardiovascular Biology and Medicine, Kings College London, London, UK

Nootropic drugs, e.g. piracetam have memory enhancing properties (Moyersoons *et al.*, 1974). They increase glucose uptake into barbiturate and benzodiazepine anaesthetised brain (Heiss *et al.*, 1988). Barbiturates and benzodiazepines inhibit glucose transport both into brain in vivo and in vitro cell systems e.g. human erythrocytes (Haspel *et al.*, 1999). We decided therefore to determine if piracetam and a neuropeptide analogue thyrotrophin releasing hormone (TRH), had antagonist effects on barbiturate and benzodiazepine-dependent inhibitions of glucose transport in human erythrocytes. Cells were loaded with 100mM glucose and exit rates of glucose from cells were monitored photometrically in the presence and absence of the drugs under test, using a fluorescence spectrometer as previously described (Naftalin *et al.*, 2004).

Pentobarbital and diazepam are mixed inhibitors of glucose transport, reducing both the V<sub>max</sub> of glucose transport and also the affinity of glucose for GLUT1. Piracetam and TRH competitively antagonise both pentobarbital or diazepam inhibition of the maximal rate of glucose exit (zero trans net exit) from erythrocytes at 25°C (K<sub>i</sub> of Piracetam =  $1.29 \pm 0.17$  mM, n=3; K<sub>i</sub> of TRH =  $132 \pm 27.8$   $\mu$ M, n=3) and decrease in glucose affinity, as measured by the infinite-cis K<sub>m</sub> (Sen-Widdas K<sub>m</sub>). A strong correlation was obtained between the observed potency of *in vivo* nootropic action of several nootropic drugs in rats and their *in vitro* K<sub>s</sub> against pentobarbital inhibition of glucose transport (n = 9, P ≤ 0.001).

Since the crystal structure of the benzodiazepine binding site to GABA A receptor is known (Sigel, 2002) we looked for similarities between amino-acid sequences in human GLUT1 and the benzodiazepine binding domains of human GABAA receptor. These homologies cluster in the N-terminal half of GLUT1. When mapped on a 3D template of GLUT1, these homologies suggest that a possible site of diazepam and piracetam interaction is a pocket outside the central hydrophilic pore region well suited to act as a non-catalytic site of inhibition (Naftalin *et al.*, 2004).

Possible position of benzodiazepine and piracetam binding site in relation 3D positions of GLUT1 transmembrane helices



A-F are regions of similarity between GLUT1 and the benzodiazepine binding site in the GABA<sub>A</sub> receptor. The rhomboid is the putative site of benzodiazepine and piracetam binding to GLUT1.

Moyersoons, F. *et al.* (1974) Arch. Int. de Pharmacodyn. Ther. **210**, 38-48.

Heiss, W.D. *et al.* (1988) *J. Cereb. Blood. Flow. Metab.*, **8**, 613-617.  
 Haspel, H.C. *et al.* (1999). *A. J. Membrane Biology*. **169**(1), 45-53.  
 Naftalin, R.J. *et al.* (2004). *Br. J. Pharmacol.* **142**, 594-608.  
 Sigel, E. (2002). *Curr. Top. Med. Chem* **2**, 833-839.

Where applicable, the experiments described here conform with Physiological Society ethical requirements.

## C3

### An electrogenic V-H<sup>+</sup>-ATPase drives electrolyte transport in the isolated perfused larval *Drosophila* midgut.

S. Shanbag and S. Tripathi

Tata Institute of Fundamental Research, Mumbai, India

Early third-instar larvae of wild-type *Drosophila* feed actively. The epithelium lining the gut is a single layer of cells, and is therefore an attractive preparation for study of nutrient and fluid and electrolyte transport. As there is considerable variation in the dimensions, cell types and transport functions along the distinct segments of the gut, we have developed an *in vitro* method for microperfusion of individual gut segments that enables independent control of solute composition of luminal and hemolymph compartments with simultaneous measurement of transepithelial potential ( $V_t$ ) and resistance ( $R_t$ ) and basolateral intracellular potential ( $V_b$ ) and ionic activities with ion-selective microelectrodes.

Midgut segments of 1 to 1.5mm length, lumen diameter 170µm and outer diameter 200µm, were dissected and perfused with isotonic insect Ringer at 23 °C. Details of the basic perfusion technique with glass micropipettes and measurement of electrical parameters have been described earlier (Tripathi & Boulpaep, 1988). Data are presented as means  $\pm$  SEM and compared by Student's t-test using paired data.

Cannulation of one end only yielded a lumen negative  $V_t$  of  $-17.8 \pm 0.4$  mV ( $n=94$ ). Simultaneous cannulation of both ends increased  $V_t$  to  $-56.8 \pm 1.0$  mV ( $n=94$ ).  $R_t$  measured by terminated cable analysis was  $719 \pm 34 \Omega \cdot \text{cm}^2$  ( $n=26$ ); the epithelium is therefore tighter than most tubular epithelia e.g. proximal renal tubules.  $V_b$  was  $-48.8 \pm 1.8$  mV ( $n=58$ ) and indicates that the apical membrane potential is of the order of 8 mV. Bilateral substitution of Cl with Gluconate changed  $V_t$  from  $-46.5 \pm 3.1$  to  $-54.5 \pm 3.7$  mV ( $n=8$ ;  $p<0.005$ ) and increased  $R_t$  from  $822 \pm 68 \Omega \cdot \text{cm}^2$  to  $2452 \pm 340 \Omega \cdot \text{cm}^2$  ( $n=8$ ;  $p<0.0001$ ). Bilateral substitution of Na with N-methyl-D-glucamine increased  $R_t$  from  $641 \pm 71 \Omega \cdot \text{cm}^2$  to  $2313 \pm 535 \Omega \cdot \text{cm}^2$  ( $n=4$ ;  $p<0.05$ ). Bilateral replacement of K with Na or  $\text{HCO}_3$  replacement with HEPES were without significant effects.

Bafilomycin A1 (a V-H-ATPase inhibitor) added to the bath to a concentration of 750 nM reduced  $V_t$  from  $-27.4 \pm 1.2$  to  $-21 \pm 1.6$  mV ( $n=3$ ;  $p<0.005$ ) without a significant increase in  $R_t$ . The inhibitory effect of bafilomycin was dose dependent and became significant at a concentration of 1µM. At 7.5µM transepithelial current was inhibited ~65% (control  $59 \pm 8 \mu\text{A} \cdot \text{cm}^{-2}$  to  $21 \pm 2 \mu\text{A} \cdot \text{cm}^{-2}$  ( $n=5$ ;  $p<0.001$ ).

We conclude that the secretion of base into the lumen by this segment is accomplished by an electrogenic V-ATPase extruding  $\text{H}^+$  to the hemolymph and is the primary driving force for electrolyte transport. The high Cl and Na permeability permits

net solute transport which would also result in net water flow across the epithelium.

Tripathi S & Boulpaep EL (1988). *Amer. J. Physiol.* **255**, F188-203.

Supported by programme 9P-821.

Where applicable, the experiments described here conform with Physiological Society ethical requirements.

## C4

### Regulation of intestinal (Caco-2) dipeptide uptake by phosphodiesterase inhibitors

C.M. Anderson and D.T. Thwaites

Institute for Cell & Molecular Biosciences, University of Newcastle upon Tyne, Newcastle upon Tyne, UK

The intestinal di/tripeptide transporter hPepT1 plays an important role in the absorption of dietary protein and peptidomimetic drugs (Rubio-Aliaga & Daniel, 2002). For optimal absorptive transport via hPepT1 an active  $\text{Na}^+/\text{H}^+$  exchanger (NHE3) is required at the brush border membrane (Thwaites *et al.* 2002). NHE3 is activated by the decrease in  $\text{pH}_i$  associated with hPepT1-mediated  $\text{H}^+$ /dipeptide symport. NHE3 extrudes protons and thus maintains the driving force (the transmembrane  $\text{H}^+$  electrochemical gradient) required for further  $\text{H}^+$ /dipeptide transport. NHE3 inhibition either by selective pharmacological inhibitors (e.g. S1611) or through activation of the cAMP/protein kinase A pathway (e.g. by vasoactive intestinal peptide) reduces hPepT1 activity indirectly via a reduction in the driving force (Anderson *et al.* 2003). The aim of this study was to investigate the effects of various phosphodiesterase inhibitors (which raise intracellular cAMP and cGMP levels by inhibiting their breakdown) on hPepT1 function. [ $^{14}\text{C}$ ]Gly-Sar uptake ( $0.5 \mu\text{Ci} \cdot \text{ml}^{-1}$ ,  $100 \mu\text{M}$ ) across the apical membrane of human intestinal Caco-2 cell monolayers (passage 100-116, 14-19 days post-seeding) was measured over 15min (apical pH 6.5, basolateral pH 7.4) in the presence and absence of various phosphodiesterase inhibitors. Caffeine and theophylline reduced Gly-Sar uptake in a concentration-dependent manner. 5mM caffeine reduced Gly-Sar uptake [mean  $\pm$  SEM ( $n$ )] from  $684 \pm 19$  to  $351 \pm 11$  ( $17-18$ )  $\text{pmol} \cdot \text{cm}^{-2} \cdot [15\text{min}]^{-1}$  ( $p<0.001$ , ANOVA, Bonferroni post test). In contrast, caffeine and theophylline (5mM) did not inhibit Gly-Sar uptake under conditions where NHE3 would be inactive e.g. in the absence of extracellular  $\text{Na}^+$ , no difference ( $p>0.05$ ) in uptake was observed ( $244 \pm 9$  and  $242 \pm 10$  ( $17-18$ )  $\text{pmol} \cdot \text{cm}^{-2} \cdot [15\text{min}]^{-1}$ ) in the absence and presence of caffeine (5mM), respectively. Pentoxifylline is a phosphodiesterase inhibitor given orally to treat intermittent claudication (Jocoby & Mohler, 2004). Pentoxifylline (5mM) inhibited Gly-Sar uptake by reducing  $V_{\text{max}}$  [from  $8246 \pm 913$  to  $5369 \pm 1167$  ( $6$ )  $\text{pmol} \cdot \text{cm}^{-2} \cdot [15\text{min}]^{-1}$  ( $p<0.05$ , Student's t-test)] without effect on affinity [ $K_m$   $1.0 \pm 0.2$  and  $1.6 \pm 0.6$  ( $6$ ) mM, ( $p>0.05$ , Student's t-test) in the presence and absence of pentoxifylline, respectively]. These observations suggest that hPepT1-mediated absorption of any drug may be reduced (following NHE3 inhibition) by phosphodiesterase inhibitors from diet or those co-administered as therapeutic agents.

Anderson CMH *et al.* (2003). *Br J Pharmacol* **138**, 564-573.

Jocoby D & Mohler ER (2004). *Drugs* **64**, 1657-1670.

Rubio-Aliaga I & Daniel H (2002). *Trends Pharmacol Sci* **23**, 434-440.  
Thwaites DT *et al.* (2002). *Gastroenterology* **122**, 1322-1333.

Supported by the BBSRC (grant 13/D17277)

Where applicable, the experiments described here conform with Physiological Society ethical requirements.

## C5

### Vigabatrin transport across the intestinal (Caco-2) apical membrane is via the human H<sup>+</sup>-coupled amino acid transporter (hPAT1)

E.L. Abbot, D.J. Kennedy, D.S. Grenade and D.T. Thwaites

School of Cell and Molecular Biosciences, University of Newcastle upon Tyne, Newcastle upon Tyne, UK

The GABA-transaminase inhibitor, gamma-vinyl-GABA (vigabatrin), has 100% oral bioavailability and is used orally to treat some forms of epilepsy (Goldsmith & de Bittencourt, 1995; Richens, 1992). There are no reports on the mechanisms involved in vigabatrin transport across the small intestinal wall. We have recently identified that the H<sup>+</sup>-coupled amino acid transporter (system PAT), characterised functionally using human intestinal Caco-2 cell monolayers (Thwaites *et al.* 2000), represents the classical "imino acid carrier" in both human and rat small intestine (Anderson *et al.* 2004). A system PAT-related cDNA clone was isolated from a Caco-2 cell cDNA library and named hPAT1 for human Proton-coupled Amino acid Transporter 1 (Chen *et al.* 2003). The purpose of this investigation was to determine the role of system PAT/hPAT1 in vigabatrin absorption. Radiolabelled uptake experiments ([<sup>3</sup>H]GABA, 20-100 μM, 0.5-5.0 μCi.ml<sup>-1</sup>) were performed using Caco-2 cell monolayers (passage no. 108-118, 14-17 days post-seeding, 15min at 37°C) and hPAT1-expressing *Xenopus laevis* oocytes (cRNA 50ng.oocyte<sup>-1</sup>, 2 days post-injection, 40min at 23°C). Under optimal transport conditions (pH 5.5, Na<sup>+</sup>-free buffers) vigabatrin (10mM) caused a significant reduction in [<sup>3</sup>H]GABA uptake (mean ± sem (n)) across the apical membrane of Caco-2 cells (from 728±76 (6) to 271±14 (6) pmol.cm<sup>-2</sup>, p<0.001, ANOVA Bonferroni post-test). Inhibition of [<sup>3</sup>H]GABA uptake via unlabelled GABA and vigabatrin had a similar concentration dependence producing IC<sub>50</sub> values of 2.1±1.4 and 2.8±1.6 mM, respectively. In hPAT1-expressing oocytes vigabatrin reduced [<sup>3</sup>H]GABA uptake by 55.8±12.3 (9) %. To determine whether vigabatrin was a transport inhibitor or substrate, substrate-induced current flow into hPAT1-expressing oocytes was measured under voltage-clamped conditions, where both GABA and vigabatrin (both 10mM) induced similar current flow (the response to vigabatrin was 75.7±6.9 (3) % (mean ± sd) of that with GABA). Similar observations were made using the GABA analogues TACA (transaminocrotonic acid) and guvacine. No current was observed in water-injected oocytes. In conclusion vigabatrin is transported across the apical membrane of Caco-2 cell monolayers via the high capacity, H<sup>+</sup>-coupled transporter hPAT1, which emphasises the potential of this transporter as a route for oral drug delivery.

Anderson CMH *et al.* (2004). *Gastroenterology* **127**, 1410-1422.

Chen Z *et al.* (2003). *J Physiol* **546.2**, 349-361

Goldsmith P & de Bittencourt PRM (1995) *Acta Neurol. Scand. Suppl.* **162**, 35-39

Richens A (1992) *Acta Neurol. Scand. Suppl.* **140**, 65-70

Thwaites DT *et al.* (2000). *Br. J. Pharmacol.* **129**, 457-464

Supported by the MRC (G9801704)

Where applicable, the experiments described here conform with Physiological Society ethical requirements.

## C6

### The *Drosophila* gene CG1139 encodes a proton-coupled amino acid transporter with functional similarity to members of the mammalian PAT (SLC36) family when expressed in *Xenopus* oocytes.

D. Meredith, D. Goberdhan, C. Wilson and C. Boyd

Human Anatomy & Genetics, University of Oxford, Oxford, UK

Sodium-independent, proton-coupled amino acid uptake at the apical membrane of the small intestine model cell line Caco-2 was originally demonstrated by Thwaites *et al.* (1993), and it is now evident that members of the SLC36 (PAT) family mediate the proton-coupled uptake of glycine, alanine and proline (reviewed by Boll *et al.* 2004). The CG1139 gene from *Drosophila melanogaster* encodes a protein with a predicted open reading frame of 451 amino acids with 33% sequence identity to both mouse PAT1 and PAT2. Here we provide evidence that CG1139 encodes a proton-coupled amino acid transport system analogous to the mammalian PAT transporters.

The CG1139 clone was obtained from the *Drosophila* Genomics Resource Centre and expressed in *Xenopus laevis* oocytes. Membrane potential and the uptake of 50 μM [<sup>3</sup>H]-Ala were measured using a similar approach to that previously described (Meredith 2004).

The membrane potential of oocytes injected with CG1139 cRNA was initially shown to depolarize in response to a mixture of 20 common L-amino acids. Further experiments revealed that the amino acids responsible for this response were alanine, glycine and proline, and that there was a larger depolarization at pH<sub>out</sub> 5.5 than 7.4 (Fig. 1A). No depolarization of membrane potential was seen in control (non-injected) oocytes. Further characterization of transport by CG1139 using 50 μM [<sup>3</sup>H]-alanine: uptake was stimulated approximately 2.5-fold by extracellular acidification (78.8 ± 2.33 versus 31.5 ± 2.41 pmoles/oocyte/hr, pH<sub>out</sub> 5.5 versus 7.4 respectively, n=5 oocytes, p<0.001 Student's t test), with an apparent K<sub>m</sub> for alanine of 1.2 ± 0.2 mM at pH<sub>out</sub> 5.5 (Figure 1B).

Thus the affinity of CG1139 for alanine falls between that of the lower affinity mouse PAT1 and the higher affinity PAT2 isoforms (K<sub>m</sub> of 7.5 and 0.26 mM respectively when expressed in *Xenopus* oocytes, Boll *et al.* 2002). We conclude that CG1139 encodes for a proton-coupled amino acid transporter with a substrate specificity for alanine, glycine and proline, similar to that of the mammalian PAT family.

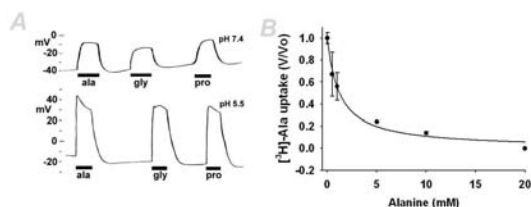


Figure 1A: Representative membrane potential recordings from a CG1139-expressing oocyte and its response to extracellular amino acids Ala, Gly and Pro (all 2mM) at pH 7.4 (upper trace) and pH 5.5 (lower trace); similar patterns of depolarisation were seen in at least 5 oocytes. Figure 1B: Self inhibition of 50μM alanine uptake at pH 5.5 (n=5 oocytes per data point,  $R^2=0.99$ ).

Thwaites DT *et al.* (1993) *JBiolChem* **268**, 18438-41.

Boll M *et al.* (2004) *Pflugers Arch* **447**, 776-9.

Meredith D (2004) *JBiolChem* **279**, 15795-8.

Boll M *et al.* (2002) *JBiolChem* **277**, 22966-22973.

We thank the Wellcome Trust, the BBSRC and Diabetes UK for their support.

Where applicable, the experiments described here conform with Physiological Society ethical requirements.

C7

### Cl<sup>-</sup> secretion induced by Ca<sup>2+</sup> agonists is impaired in distal colon of a *Kcnn4* null mouse

C.A. Flores<sup>1</sup>, J.E. Melvin<sup>2</sup> and F.V. Sepulveda<sup>1</sup>

<sup>1</sup>Centro de Estudios Científicos, (CECS), Valdivia, Chile and <sup>2</sup>Center for Oral Biology in the Aab Institute for Biomedical Sciences, University of Rochester Medical Center, Rochester, NY, USA

Ca<sup>2+</sup>-dependent anion secretion in distal colon requires the simultaneous activity of apical CFTR Cl<sup>-</sup> channels activated by cAMP and basolateral (BL) K<sup>+</sup> channels activated by Ca<sup>2+</sup>. Three classes of Ca<sup>2+</sup>-activated K<sup>+</sup> channels have been distinguished from their single channel conductances. The small-, intermediate-, and large-conductance channels SK, IK, and BK, respectively. SK channels are encoded by three genes, *Kcnn1-3*, IK and BK channels are the products of the *Kcnn4* and *Slo* (*Kcnnal*) genes, respectively. Ca<sup>2+</sup>-activated K<sup>+</sup> channels of all three types have been identified in the colon and could participate in Ca<sup>2+</sup>-dependent anion secretion. We have now used an animal deficient in IK1, the *Kcnn4* null mouse (Begenesich *et al.*, 2004), to test for its participation in this process.

A piece of distal colon was gently stripped of the muscle layer, placed in an Ussing chamber (0.1 cm<sup>2</sup>) in a bicarbonate buffered solution, gassed with 95% O<sub>2</sub>/5% CO<sub>2</sub> at 37°C. The transepithelial potential difference was monitored continuously and 20 μA pulses were passed to calculate tissue resistance and equivalent short circuit current (Isc). To induce cAMP-mediated Cl<sup>-</sup> secretion tissues were incubated with 100 μM IBMX and 1 μM forskolin. Chromanol 293 B (10 μM) was added at the BL side to close KCNQ1/KCNE3 K<sup>+</sup> channels. BL carbachol (CCh, 100 μM) was used as Ca<sup>2+</sup> agonist. Clotrimazol (3 μM) and Ba<sup>2+</sup> (5 mM) were used as K<sup>+</sup> channel blockers. For K<sup>+</sup> secretion experiments, tissues were incubated with indomethacin (2 μM) pre-

vious to CCh application, to avoid basal release of prostaglandin and consequent cAMP increase.

Wild type (WT) and knockout (KO) animals had cAMP-induced Cl<sup>-</sup> secretion of similar magnitude ( $\Delta$ Isc -149 ± 21 and -144 ± 11 μA cm<sup>-2</sup>, means ± SEM, n=5 & 4 respectively). When CCh was added, only WT tissues had a current response consistent with Ca<sup>2+</sup> dependent Cl<sup>-</sup> secretion ( $\Delta$ Isc = -174 ± 12 μA cm<sup>-2</sup>), which was decreased by the IK1 inhibitor clotrimazol ( $\Delta$ Isc = -38 ± 3.6 μA cm<sup>-2</sup>, n=5, p<0.0005). In KO tissues, CCh induced positive Isc change ( $\Delta$ Isc 17 ± 6 μA cm<sup>-2</sup>, n=4) consistent with K<sup>+</sup> secretion, which was inhibited by apical Ba<sup>2+</sup> ( $\Delta$ Isc 8.7 ± 1.8 μA cm<sup>-2</sup>, n=3, p<0.05), but not by clotrimazol ( $\Delta$ Isc 19 ± 7 μA cm<sup>-2</sup>, n=3). Experiments with epithelia treated with indomethacin suggest that both WT and KO tissues are able to secrete K<sup>+</sup> under CCh stimulation. This was inhibited by Ba<sup>2+</sup> but not affected by clotrimazol.

Our data suggests that IK1 encoded by the *Kcnn4* gene is the main Ca<sup>2+</sup>-activated K<sup>+</sup> channel that drives Cl<sup>-</sup> secretion by Ca<sup>2+</sup> agonists in mouse distal colon. They also suggest that a different, as yet unidentified Ba<sup>2+</sup>-sensitive apical K<sup>+</sup> channel mediates CCh-activated K<sup>+</sup> secretion.

Begenesich, T. *et al.* (2004) *J. Biol. Chem* doi 10.1074/jbc.M409627200

CAF is a PhD student at the Universidad Austral de Chile.

Where applicable, the experiments described here conform with Physiological Society ethical requirements.

C8

### Non-oxidative metabolites of ethanol deplete endoplasmic reticulum (ER) Ca<sup>2+</sup> stores in mouse pancreatic acinar cells

D.N. Criddle<sup>1</sup>, G. Fistetto<sup>1</sup>, M.G. Raraty<sup>2</sup>, J.P. Neoptolemos<sup>2</sup>, A.V. Tepikin<sup>1</sup>, O.H. Petersen<sup>1</sup> and R. Sutton<sup>2</sup>

<sup>1</sup>Department of Physiology, University of Liverpool, Liverpool, UK and <sup>2</sup>Department of Surgery, University of Liverpool, Liverpool, UK

Recently we have shown that non-oxidative ethanol metabolites elicit a sustained rise in the cytosolic Ca<sup>2+</sup> concentration ([Ca<sup>2+</sup>]<sub>i</sub>), causing pancreatic acinar cell damage (Criddle *et al.* 2004). We have now investigated the mechanisms by which ethanol and its metabolites influence cellular Ca<sup>2+</sup> homeostasis using confocal microscopy.

Experiments were carried out in freshly dispersed mouse pancreatic acinar cells (singlet, doublet or triplets) and results are expressed as mean ± s.e.m. Ethanol (850 mM) produced only small, sustained increases in [Ca<sup>2+</sup>]<sub>i</sub> (115 ± 12 nM) in the majority of cells (68%), whilst in the remainder a sharp, transient 'spike' increase in [Ca<sup>2+</sup>]<sub>i</sub> (533 ± 30 nM) was observed that declined to a similarly low resting level. In contrast, large and sustained (≥20 min) rises in [Ca<sup>2+</sup>]<sub>i</sub> of 546 ± 36 nM (n=34) and 557 ± 46 nM (n=12) were induced by the non-oxidative ethanol metabolite palmitoleic acid ethyl ester (POAEE; 100 μM; with 850 mM ethanol to maintain solubility) and palmitoleic acid (POA; 100 μM, in the absence of ethanol), respectively. The increases in [Ca<sup>2+</sup>]<sub>i</sub> induced by 850 mM ethanol, 100 μM POAEE or 50 μM POA were not inhibited by 50 μM ryanodine or 20 mM caffeine (n=6-8; p>0.05 ANOVA), indicating that neither ryanodine receptors (RyRs) nor inositol trisphosphate receptors

(IP<sub>3</sub>Rs) were involved. Under Ca<sup>2+</sup>-free conditions, prior release of ER Ca<sup>2+</sup> stores with 2  $\mu$ M thapsigargin or 10  $\mu$ M acetylcholine abolished subsequent increases in [Ca<sup>2+</sup>]<sub>i</sub> by 50  $\mu$ M POA and vice versa (n=17). Direct measurements of the ER Ca<sup>2+</sup> concentration showed that both POAEE (100  $\mu$ M) and POA (50  $\mu$ M) emptied the ER stores (n=10), in contrast to time-control experiments in the absence of ethanol metabolites (n=16), and also markedly reduced NADH autofluorescence. POA induced complete mitochondrial depolarization, measured with tetramethyl rhodamine methyl ester (n=9). We conclude that non-oxidative ethanol metabolites increase [Ca<sup>2+</sup>]<sub>i</sub>, primarily via Ca<sup>2+</sup> release from the ER, independently of RyRs or IP<sub>3</sub>Rs. Mitochondrial ATP depletion may be an important causal factor. These actions of the non-oxidative ethanol metabolites are most likely the principal means whereby ethanol induces acute pancreatitis.

Criddle DN et al. (2004). *Proc. Natl. Acad. Sci. USA*. 101: 10738-43.

This work was funded by the Medical Research Council

Where applicable, the experiments described here conform with Physiological Society ethical requirements.

## C9

### The effect of phenformin on short-circuit current ( $I_{sc}$ ) across H441 human lung epithelial cells

A. Woollhead<sup>1</sup>, J. Scott<sup>2</sup> and D. Baines<sup>1</sup>

<sup>1</sup>Basic Medical Sciences, St George's Hospital Medical School, London, UK and <sup>2</sup>Molecular Physiology, Wellcome Trust Biocentre, Dundee, UK

Active reabsorption of Na<sup>+</sup> across the alveolar epithelium is essential for lung fluid homeostasis. Na<sup>+</sup> entry at the apical membrane of the lung epithelial cell is predominantly via the amiloride-sensitive Na<sup>+</sup> channel (ENaC) down its electrochemical gradient. This gradient is generated and maintained by Na<sup>+</sup> extrusion via the Na<sup>+</sup>K<sup>+</sup>ATPase pump located at the basolateral membrane.

Phenformin, an oral hypoglycaemic biguanide has been shown to influence cellular metabolism and membrane function. This has recently been attributed, in part, to its ability to activate AMP-activated protein kinase (AMPK) (Sakamoto et al. 2004). Therefore, we explored the effect of phenformin and activation of AMPK on ion transport across H441 human lung epithelial cells.

H441 cells were cultured on permeable supports for 7 days and monolayers were treated both apically and basolaterally with 10mM phenformin for 1 hour. Monolayers were then mounted in Ussing chambers where phenformin was circulated in physiological saline throughout the course of the experiment. Spontaneous short circuit current ( $I_{sc}$ ) was measured by clamping transepithelial voltage ( $V_t$ ) at zero. Statistical analysis was carried out using Student's t-test where p values of < 0.05 were considered significant. Data are presented as mean  $\pm$  SEM

Treatment with phenformin resulted in a significant decrease in spontaneous  $I_{sc}$  ( $18.9 \pm 2.29 \mu A.cm^{-2}$ ) compared to that of controls ( $42.3 \pm 1.8 \mu A.cm^{-2}$ ,  $p < 0.001$ ,  $n = 4$ ). This was not the result of differences in the resistive properties between treated and untreated monolayers ( $p = 0.33$ ,  $n = 4$ ). Forskolin (10  $\mu$ M) induced a rise in  $I_{sc}$  of  $13.8 \pm 4.2 \mu A.cm^{-2}$  in control cells which was not evident in the presence of phenformin ( $0.2 \pm 0.32 \mu A.cm^{-2}$   $p <$

0.05,  $n = 3$ ). Application of 10  $\mu$ M amiloride to the monolayers showed that phenformin significantly reduced the amiloride-sensitive component of  $I_{sc}$  ( $14.3 \pm 1.3 \mu A.cm^{-2}$ ) compared to control ( $46.9 \pm 4.9 \mu A.cm^{-2}$   $p < 0.01$ ,  $n = 3$ ). Na<sup>+</sup>K<sup>+</sup>ATPase pump capacity was determined by apical permeabilisation with 75  $\mu$ M nystatin followed by blockade with 100  $\mu$ M ouabain. Ouabain-sensitive current was also significantly reduced in phenformin treated cells ( $12.3 \pm 0.3 \mu A.cm^{-2}$ ) compared to that of controls ( $39.4 \pm 6.2 \mu A.cm^{-2}$   $p = 0.01$ ,  $n = 3$ ). Phenformin induced a 3.8-fold rise in AMPK activity in H441 cells from  $0.5 \pm 0.1$  to  $1.8 \pm 0.2 \text{ nmol min}^{-1} \text{ mg}^{-1}$  ( $p = 0.001$ ,  $n = 4$ ). Taken together these data indicate that 10mM phenformin suppresses amiloride-sensitive Na<sup>+</sup> transport across H441 cells via a pathway that includes activation of AMPK and inhibition of Na<sup>+</sup>K<sup>+</sup>ATPase.

Sakamoto K et al. (2004) *Am J Physiol Endocrinol Metab* 287(2): E310-7.

Funded by the Wellcome Trust.

Where applicable, the experiments described here conform with Physiological Society ethical requirements.

## C10

### Ca<sup>2+</sup>-evoked membrane currents in a cell line (H441) derived from the human bronchial epithelium

R.P. McNeill, M.T. Clunes, L.A. Chambers and S.M. Wilson

TICH, University of Dundee, Dundee, Tayside, UK

H441 cells express an amiloride-sensitive Na<sup>+</sup> conductance ( $G_{Na}$ ) similar to that associated with co-expression of the epithelial Na<sup>+</sup> channel (ENaC)  $\alpha$ ,  $\beta$  and  $\gamma$  subunits, and regulated increases in  $G_{Na}$  seem to underlie the cAMP-evoked stimulation of Na<sup>+</sup> transport seen in these cells (Clunes et al., 2004). However, as well as increasing [Ca<sup>2+</sup>]<sub>i</sub>, thapsigargin (1  $\mu$ M) also increases the short circuit current recorded from these cells ( $\Delta I_{sc} = 24.3 \pm 2.4 \mu A.cm^{-2}$ ,  $n = 6$ ,  $P < 0.01$ ), suggesting that Na<sup>+</sup> transport is also controlled via [Ca<sup>2+</sup>]<sub>i</sub>. This was unexpected as Ca<sup>2+</sup> is thought to inhibit ENaC (Ishikawa et al., 1998) and so, to establish the physiological basis of this response, we explored the effects of thapsigargin (1  $\mu$ M) upon the membrane currents recorded from groups of 2-5 cells (Clunes et al., 2004).

Thapsigargin consistently evoked Ca<sup>2+</sup>-dependent membrane currents (Fig 1A) and the current recorded from thapsigargin-treated cells reversed at a potential close to  $E_K$  (Fig 1B). This Ca<sup>2+</sup>-mobilising agent had thus increased  $G_K$  and further analysis showed that this was associated with a hyperpolarization of  $V_m$  (control:  $-50 \pm 6 \text{ mV}$ ; thapsigargin:  $-78 \pm 1 \text{ mV}$ ,  $P < 0.01$ ). We also studied the effects of thapsigargin upon  $G_{Na}$  by characterising amiloride-sensitive currents in cells treated with clotrimazole (1  $\mu$ M) which was shown to block the thapsigargin-evoked increase in  $G_K$  (Clunes et al., 2005). These experiments confirmed the expression of a selective Na<sup>+</sup> conductance and showed that the magnitude of this conductance increased slightly during exposure to thapsigargin (control:  $157 \pm 16 \text{ pS cell}^{-1}$ ; thapsigargin:  $267 \pm 24 \text{ pS cell}^{-1}$ ,  $n = 7$ ,  $P < 0.02$ ) a result that contrasts with earlier work (Ishikawa et al., 1998). Thapsigargin may thus stimulate Na<sup>+</sup> transport by (i) hyperpolarising  $V_m$  and increasing the driving force for Na<sup>+</sup> entry and (ii) increasing  $G_{Na}$  by an unknown mechanism.

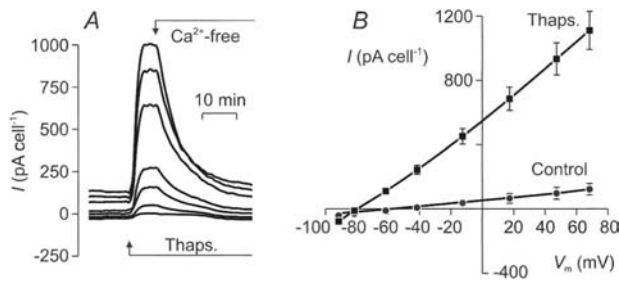


Fig. 1. Dexamethasone-treated (0.2  $\mu$ M) H441 cells grown on glass coverslips were held under voltage clamp in the perforated patch recording configuration. The membrane currents were evoked by driving  $V_m$  through a series of 7 steps ( -90 mV to +68 mV; holding potential -40 mV) every 15 s and A shows the effects of thapsigargin upon the currents recorded at each such potential;  $\text{Ca}^{2+}$  was removed from the external solution as indicated. B Whole cell current voltage relationship (mean  $\pm$  s.e.m.,  $n = 9$ ) in control and thapsigargin-treated cells.

Clunes, M. T., Butt, A. G. & Wilson, S. M. (2004). *J. Physiol. Lond.* 557, 809-819.

Clunes, M. T., McNeill, R. P. & Wilson, S. M. (2005). *Proc. Physiol. Soc. King's College London Meeting*.

Ishikawa, T., Marunaka, Y. & Rotin, D. (1998). *J. Gen. Physiol.* 111, 825-846.

*Where applicable, the experiments described here conform with Physiological Society ethical requirements.*

C122

### Increased transepithelial $\text{Na}^+$ transport due to the activation of an intermediate conductance $\text{K}^+$ ( $\text{I}_\text{K}$ ) channel in H441 airway epithelial cells.

M.T. Clunes, R.P. McNeill and S.M. Wilson

TICH, University of Dundee, Dundee, Tayside, UK

Thapsigargin evokes increased  $\text{Na}^+$  transport in H441 cells and, at least in part, this response is due to a  $\text{Ca}^{2+}$ -dependent increase in  $\text{K}^+$  conductance ( $G_\text{K}$ ) (McNeill et al., 2005). To characterise the channels underlying this response, we have now explored the effects of putative  $\text{K}^+$  channel blockers upon the thapsigargin-evoked increase in membrane current.  $\text{Ba}^{2+}$  (5 mM) caused  $73 \pm 8\%$  inhibition whilst 1  $\mu\text{M}$  clotrimazole essentially abolished the response ( $97 \pm 5\%$ ) and, since apamin (1  $\mu\text{M}$ ,  $n = 4$ ) and iberiotoxin (0.1  $\mu\text{M}$ ,  $n = 7$ ) were ineffective, this suggests that the thapsigargin-evoked increase in  $G_\text{K}$  (McNeill et al., 2005) reflects increased activity of  $\text{K}^+$  channels belonging to the  $\text{I}_\text{K}$  family. Further evidence of this came from RT-PCR based studies which showed that H441 cells expressed  $\text{I}_\text{K}$  channel mRNA transcripts but did not express either the large or small conductance  $\text{K}^+$  channel. Moreover, 1 mM EBIO, a substance that characteristically activates  $\text{I}_\text{K}$  channels, caused an increased in membrane conductance (control:  $353 \pm 68 \text{ pS cell}^{-1}$ , EBIO:  $1222 \pm 245 \text{ pS cell}^{-1}$ ) that reflected activation of a  $\text{K}^+$  selective current and which caused a hyperpolarization of  $V_\text{m}$  (control:  $-52 \pm 3 \text{ mV}$ ; EBIO:  $-79 \pm 1 \text{ mV}$ ,  $P < 0.001$ ). These data suggest that the thapsigargin-evoked increase in  $I_\text{SC}$  (McNeill et al., 2005) is due to increased activity of  $\text{I}_\text{K}$  channels, a hypothesis that predicts that EBIO-evoked activation of these channels will mimic the electrometric response to thapsigargin. We therefore explored the effects of EBIO upon  $I_\text{SC}$  and  $[\text{Ca}^{2+}]_\text{i}$  measured simultaneously in polarised H441 cells (Fig 1). As anticipated, EBIO increased  $I_\text{SC}$  without affecting  $[\text{Ca}^{2+}]_\text{i}$  and so the present data suggest that  $\text{Ca}^{2+}$  mobilising agonists could be important regulators of epithelial  $\text{Na}^+$  transport in some tissues.

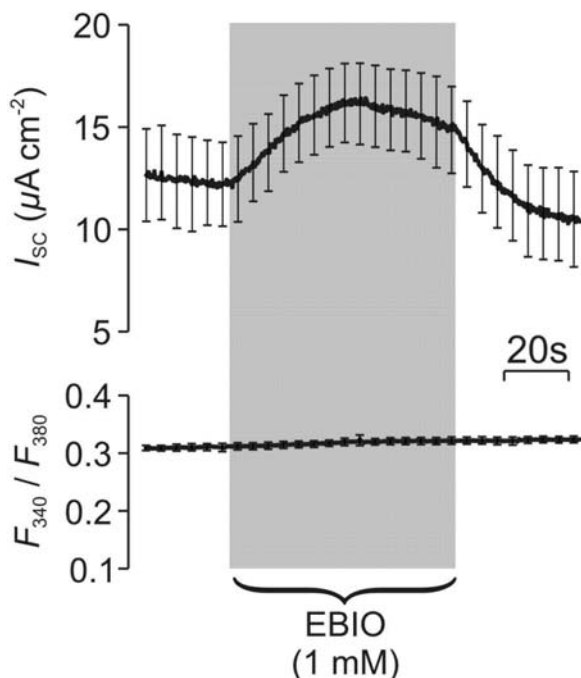


Fig. 1. H441 cells grown to confluence on permeable membranes were grown to confluence (5 days) on permeable membranes; loaded with Fura-2 and mounted in a miniature Ussing chamber so that short circuit current ( $I_\text{SC}$ , upper trace) and Fura-2 fluorescence ratio (lower trace) could be monitored simultaneously (mean  $\pm$  s.e.m.,  $n = 6$ ) whilst the apical and basolateral compartments were independently superfused with physiological salt solution. EBIO was present throughout the period indicated by the shaded bar.

McNeill, R. P., Clunes, M. T., Chambers, L. A. & Wilson, S. M. (2005). Proc. Physiol. Soc. King's College London Meeting.

Where applicable, the experiments described here conform with Physiological Society ethical requirements.

C123

### Dexamethasone treatment improves intestinal function and vascular permeability post abdominal irradiation in mice

P. Monti, A. Van der Meeren, J. Wysocki and N.M. Griffiths

DRPH, Institut de Radioprotection et de Surete Nucleaire, Fontenay aux Roses, France

Damage to the gut appears to have a motor role in the development of multiple organ failure (MOF) in cases of severe injury such as septic shock or ionising radiation exposure. Current theories suggest that intestinal damage is associated with the initiation and maintenance of systemic inflammatory-anti-inflammatory responses. One anti-inflammatory therapeutic approach for MOF remains the use of corticosteroids. However the real benefits of these agents are under continual reappraisal. The objective of the present study was to investigate intestinal and vascular function and inflammatory reactions following abdominal irradiation in mice treated or not with the synthetic corticosteroid, Dexamethasone (Dex).

Mice (male C57BL/6J) were anaesthetised (xylazine 20 mg kg<sup>-1</sup>; ketamine 50 mg kg<sup>-1</sup> i.p.) and exposed to a total abdominal irradiation (15 Gy, X, 2 Gy/min). Dex treatment (3 mg kg<sup>-1</sup> i.p.) was started 2h post exposure and continued for 3 days (functional studies) or 14 days for survival studies with decreased dose from day 7. Animals received antibiotic treatment from day 1 (Baytril, 60 mg kg<sup>-1</sup>, p.o.). At 4 days animals were anaesthetised for in vivo measurement of intestinal (jejunal closed loop) or vascular (intra-vital microscopy) FITC-dextran permeability. Tissues were removed from another group after animals were humanely killed by exsanguination for histological and biochemical analyses.

At this dose of irradiation animals lost around 25-30% body weight concomitant with a reduction of food and water intake and a 7-day survival rate of 50%. At 4 days post exposure intestinal structure was severely modified (crypt loss, oedema, inflammatory cell infiltrate) in parallel with increased intestinal cytokine levels TNF $\alpha$ , IL-6, KC ( $p < 0.05$ ,  $N = 6$ ). Intestinal permeability increased 3 fold and intestinal enzyme activities (sucrase, Na,K-ATPase) were markedly reduced ( $\sim 50\%$ ). Vascular permeability index (p.i) was increased from  $41.2 \pm 4.5$  (controls  $N = 4$ ) to  $83.2 \pm 9.7$  (irradiated  $N = 4$ ). Dex treatment increased survival (100%) and improved intestinal structure, enzyme activity (sucrase 0 Gy  $0.34 \pm 0.14$ , 15Gy  $0.18 \pm 0.01$ , 15 Gy + Dex  $0.31 \pm 0.03$   $N = 14$ ) and vascular permeability (p.i.  $44.6 \pm 9.5$   $N = 4$ ). However gut permeability remained higher

in Dex-treated animals. Tissue KC levels were reduced by Dex treatment (~30%). In conclusion, this study provides evidence of a gut inflammatory response concomitant with modifications of gut function post abdominal irradiation and dexamethasone treatment improved survival and intestinal function. All procedures accord with current national and local guidelines.

Financial support gratefully acknowledged from Delegation Generale des Armees

Where applicable, the experiments described here conform with Physiological Society ethical requirements.

C124

### Mechanism of thromboxane A<sub>2</sub>-stimulated cell proliferation of human colonic cancer cells

H. Sakai<sup>1</sup>, T. Suzuki<sup>1</sup>, N. Horikawa<sup>2</sup>, M. Ukai<sup>1</sup>, K. Tauchi<sup>2</sup>, T. Minamimura<sup>2</sup>, Y. Tabuchi<sup>3</sup>, M. Morii<sup>1</sup>, K. Tsukada<sup>2</sup> and N. Takeguchi<sup>1</sup>

<sup>1</sup>Department of Pharmaceutical Physiology, Toyama Medical and Pharmaceutical University, Toyama, Japan, <sup>2</sup>Department of Surgery II, Toyama Medical and Pharmaceutical University, Toyama, Japan and <sup>3</sup>Life Science Research Centre, Toyama Medical and Pharmaceutical University, Toyama, Japan

Tumor growth of colorectal cancers accompanies up-regulation of inducible cyclooxygenase-2, which catalyzes a key step in conversion of arachidonic acid to prostaglandin H<sub>2</sub> (PGH<sub>2</sub>) (Marx, 2001). In the downstream of COX, thromboxane synthase (TXS) catalyzes the conversion of PGH<sub>2</sub> to thromboxane A<sub>2</sub> (TXA<sub>2</sub>). We found recently that TXS is significantly up-regulated in the human colorectal carcinomas (Sakai *et al.* 2003). TXS was also highly expressed in human colonic cancer cell lines. Disruption of TXS protein by the antisense oligonucleotide inhibited the proliferation of the cancer cells (Suzuki *et al.* 2004). Herein we investigated if the K<sub>v</sub>7.1 (K<sub>LQT1</sub>), a voltage-dependent K<sup>+</sup> channel, is involved in the TXA<sub>2</sub>-induced cell proliferation. Human colorectal cancer tissue and its accompanying normal mucosa were obtained from surgical resection of Japanese patients in accordance with the recommendations of the Declaration of Helsinki and with the ethics committee approval. The expression of K<sub>v</sub>7.1 protein in human tissues and human colonic carcinoma cell lines was examined by Western blotting. Cell proliferation assay was performed by counting the number of the cell in a 12-well plate. Results are shown as means ± S.E.M. The data were statistically analysed using one-way ANOVA and Tukey's multiple comparison test.

We compared the expression levels of K<sub>v</sub>7.1 protein between human colorectal cancer tissue and its accompanying normal mucosa. It was found that K<sub>v</sub>7.1 is up-regulated in human cancer tissues (70 kDa; 10 of 10 cases, 100%). Significant expression of K<sub>v</sub>7.1 protein was also observed in the human colonic cancer cell lines such as KM12-L4, HT-29, T-84, WiDr (*n* = 3). A stable analog of TXA<sub>2</sub> (STA<sub>2</sub>; 0.1 μM) stimulated the proliferation of KM12-L4 cells from (1.31 ± 0.03) × 10<sup>5</sup> to (1.65 ± 0.04) × 10<sup>5</sup> cells (*n* = 5, *P* < 0.01), and the STA<sub>2</sub>-induced effect was completely inhibited by chromanol 293B (10 μM), an inhibitor of K<sub>v</sub>7.1 (*n* = 5, *P* < 0.01). STA<sub>2</sub> (0.1 μM) significantly

increased the expression level of K<sub>v</sub>7.1 protein by (2.09 ± 0.09)-fold in the KM12-L4 cells (*n* = 4, *P* < 0.01). In the cells, STA<sub>2</sub> also increased the chromanol 293B-sensitive K<sup>+</sup> current from 8.87 ± 1.01 to 16.91 ± 1.25 pA pF<sup>-1</sup> at +30 mV (*n* = 7, *P* < 0.01). These results suggest that paralleled up-regulations of TXS and K<sub>v</sub>7.1 channel may be involved in the tumor growth of human colorectum.

Marx J (2001) *Science* **291**, 581-582.

Sakai H *et al.* (2003). *J Physiol* **547P**, C113.

Suzuki T *et al.* (2004). *J Physiol* **555P**, C114.

Where applicable, the experiments described here conform with Physiological Society ethical requirements.

C125

### Low extracellular pH protects mouse macrophages against apoptosis induced by oxidised low density lipoprotein under normoxic or hypoxic conditions

D. Peiris<sup>1</sup>, A.B. Gerry, G.E. Mann<sup>2</sup> and D.S. Leake<sup>1</sup>

<sup>1</sup>Cardiovascular Research Group, School of Animal and Microbial Sciences, University of Reading, Reading, UK and <sup>2</sup>Cardiovascular Division, King's College London, London, SE1 1UL, UK

Atherosclerotic lesions are hypoxic (Bjornheden *et al.* 1999) and have a low extracellular pH (Naghavi *et al.* 2002) (probably in co-existence) compared to the normal intima of an artery. Oxidised low density lipoprotein (LDL) is believed to be involved in atherosclerosis and apoptosis of macrophages occurs in atherosclerotic lesions. We have therefore investigated the effects of pH and hypoxia on apoptosis induced by oxidised LDL in macrophages.

Human LDL was oxidised by dialysis for 24 h against 10 μM CuSO<sub>4</sub> at 37°C and contained high levels of oxysterols and only low levels of lipid hydroperoxides (as they had largely decomposed). Murine J774 macrophages were cultured in the absence or presence of oxidised LDL (100 μg protein/ml) at 3% oxygen (hypoxia) or 20% oxygen (normoxia for cell cultures) at pH 7.4 or 7.0 for 18 h. Flow cytometry was used to measure apoptosis (annexin V binding) and necrosis (propidium iodide uptake). Oxidised LDL was damaging for most cells, causing a large increase in apoptosis and secondary necrosis (apoptosis followed by necrosis) of the macrophages at pH 7.4 under normoxic or hypoxic conditions. Low extracellular pH had a marked protective effect against cell death induced by oxidised LDL (decreasing apoptosis plus secondary necrosis) under both oxygen levels (78.5 ± 6.0% at pH 7.4 vs. 44.8 ± 5.3% at pH 7.0 for normoxia; mean ± SEM, *n* = 17 individual experiments, *P* < 0.001). The healthy cell population increased from 15.8 ± 3.7% at pH 7.4 to 52.2 ± 5.2% at pH 7.0 (*P* < 0.001). Similar effects were observed when the extracellular pH was lowered under hypoxic conditions. We conclude that low extracellular pH in atherosclerotic lesions may protect macrophages against the cytotoxic effects of oxidised LDL under both normoxic and hypoxic conditions.

Bjornheden, T. *et al.* (1999) *Arterioscler. Thromb. Vasc. Biol.* **19**, 870-876.

Naghavi, M. *et al.* (2002). *Atherosclerosis* **164**, 27-35.

Supported by the Wellcome Trust.



Where applicable, the experiments described here conform with Physiological Society ethical requirements.

C126

### Role of neurotrophic factors (NTF) and extracellular matrix components (ECM) on VIP expression in the rat enteric nervous system (ENS)

O. Xeniou, I.A. Romero and M.J. Saffrey

Biological Sciences, Open University, Milton Keynes, UK

We studied changes in vasoactive intestinal peptide (VIP) and neuronal nitric oxide synthase (nNOS) expression by myenteric neurons during early postnatal development in parallel with maturation of the environment of myenteric neurons, specifically the expression of ECM components and NTF. Although these molecules are known to promote neuronal differentiation [Shetty & Turner, 1998; Sieber-Blum et al. 1981], very little is known about their role in the early postnatal ENS.

Sprague-Dawley rats were killed by cervical dislocation. The ileal muscularis externa, including myenteric ganglia, was processed for semi-quantitative RT-PCR at postnatal days P1, P7 and P21 (internal standards:  $\beta$ III tubulin and PGP9.5). VIP (Fig. 1), nNOS and NT-3 mRNA levels showed a consistent increase between P1 and P21. Although no changes in GDNF mRNA levels were observed, there was an increase in levels of mRNA of its co-receptor, GFR $\alpha$ -1, indicating that the responsiveness of myenteric neurons to GDNF might be enhanced at older ages. Immunofluorescent labelling of ileal cross sections revealed changes in the levels of laminin (peak at P7) and fibronectin (peak at P21).

Next, we tested the effect of ECM and NTF on myenteric neurons in cultures of dissociated myenteric ganglia (P7/8) [Schafer et al. 1997]. Changes in cell numbers per unit area of coverslips were measured after double labelling for  $\beta$ III tubulin and VIP. GDNF, but not NT-3 or BDNF (all at 1 ng/ml), enhanced survival of the overall neuronal population (35-67% increase,  $n=3$  experiments,  $P<0.02$ , paired t-test) and the percentage of VIP positive neurons (39-59%,  $n=3$ ,  $P<0.02$ ). Elevation of VIP and nNOS mRNA levels after treatment with GDNF was confirmed by RT-PCR. The effect of GDNF on neuronal survival was maintained in the presence of laminin (26-58% increase,  $n=3$ ,  $P<0.05$ ) and fibronectin (34-55%,  $n=3$ ,  $P<0.012$ ), although neither factor alone influenced neuronal survival. Fibronectin (10-18% increase,  $n=3$ ,  $P=0.10$ ), but not laminin (19-81% increase,  $n=3$ ,  $P<0.04$ ), reduced the effect of GDNF on the proportion of VIP positive neurons.

Our study suggests that GDNF regulates VIP and nNOS expression by myenteric neurons. Fibronectin was found to influence the effect of GDNF on VIP phenotype. Together with the observed changes in the environment of myenteric neurons in the early postnatal gut, our results indicate that both NTF and ECM components are likely to contribute to postnatal development of the ENS.

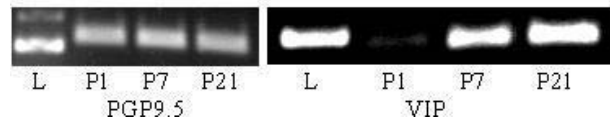


Fig. 1. Increase in VIP mRNA levels between P1-P21 (internal standard PGP9.5; L: Ladder).

Shetty, A. K. and Turner, D. A. (1998). J Neurobiol. 35 (4): 395-425.

Sieber-Blum, M., et al (1981). Exp Cell Res. 133 (2): 285-95.

Schafer, KH, et al. (1997). Brain Research Protocols, 1:109-113.

Where applicable, the experiments described here conform with Physiological Society ethical requirements.

C127

### Can the Na<sup>+</sup> pump mediate passive cation movements in the absence of ATP and P<sub>i</sub>?

J.D. Cavieres and M. Taylor

Cell Physiology & Pharmacology, University of Leicester, Leicester, UK

We have been using ATP analogues to try and map two ATP binding sites in the  $\alpha$  subunit of pig kidney Na,K-ATPase (Cavieres, 2000; Ward & Cavieres, 1998, 2003). In the native enzyme, TNP-8N<sub>3</sub>-[ $\alpha^{32}$ P]-ADP anchors at  $\alpha$ Lys480, near the FITC site; the FITC-enzyme incorporates the radioactive analogue at a downstream site instead. Here we focus on the conditions for photoinactivating and labelling both native and FITC-modified Na,K-ATPase with TNP-8N<sub>3</sub>-ADP, specially the effects of Na<sup>+</sup> and K<sup>+</sup>.

The native sodium pump can be photoinactivated by TNP-8N<sub>3</sub>-ADP in the presence of just 50 mM Tris/Cl<sup>-</sup> (pH 7.5), 1 mM EDTA. The rate constant ( $k_{\text{inact}}$ ) increases hyperbolically with  $k_{\text{inact(max)}} = 0.054 \pm 0.002 \text{ min}^{-1}$  and  $K_{\text{D(TNP-8N}_3\text{-ADP)}} = 0.11 \pm 0.02 \mu\text{M}$  (mean  $\pm$  S.E.); ATP and TNP-ATP protect with high affinities. Addition of Na<sup>+</sup> does not affect  $k_{\text{inact}}$  but K<sup>+</sup> decreases it, with  $K_{0.5(\text{K})} = 12 \pm 4 \mu\text{M}$ . Sodium ions reverse the K<sup>+</sup> effect, and  $K_{0.5(\text{Na})}$  is  $0.58 \pm 0.08 \text{ mM}$  at  $30 \mu\text{M K}^+$ . All this is to be expected, as both native and FITC-modified Na,K-ATPase spontaneously adopt an E1 or "Na<sup>+</sup> form", whilst K<sup>+</sup> causes a conformational shift towards a "K<sup>+</sup>-occluded form", both cations acting at intracellular sites (Rephaeli *et al.*, 1986). In the FITC-enzyme the surviving K<sup>+</sup>-phosphatase and P<sub>i</sub>-phosphorylation reactions cannot be photoinactivated in the presence of Tris alone, not even at 200-fold higher TNP-8N<sub>3</sub>-ADP concentrations. In this case, Na<sup>+</sup> promotes photoinactivation hyperbolically with similar  $k_{\text{inact(max)}}$  but with  $K_{0.5(\text{Na})} = 97 \pm 9 \text{ mM}$ ; K<sup>+</sup> counters this effect with  $K_{0.5(\text{K})} = 2.5 \pm 0.6 \text{ mM}$  (Ward & Cavieres, 1998). As the intracellular Na<sup>+</sup> and K<sup>+</sup> affinities in the FITC-enzyme are similar to those in native Na,K-ATPase (Rephaeli *et al.*, 1986), the latter Na<sup>+</sup> and K<sup>+</sup> effects can only be attributed to an external cation site. The hyperbolic Na<sup>+</sup> activation may result from occupation of the "third external Na<sup>+</sup> site" (Cavieres & Ellory, 1975).

It is then possible that Na,K-ATPase can shuttle K<sup>+</sup> (and Na<sup>+</sup>?) plus unloaded cation sites in the absence of ATP and P<sub>i</sub>; the forms that react with TNP-8N<sub>3</sub>-ADP would be E1 (or E1·Na<sub>i</sub><sup>+</sup>) and E2·Na<sub>o</sub><sup>+</sup> in the native and FITC-modified enzymes, respectively.

To be commensurate with  $k_{\text{inact(max)}}$ , the slippage needs to be about 0.02% of the active transport rate.

Cavieres JD (2000). J. Physiol. 523.P, 56S

Cavieres JD & Ellory JC (1975). Nature 255, 338-340

Rephaeli A, Richards D & Karlish SJD (1986). J. Biol. Chem. 261, 6248-6254

Ward DG & Cavieres JD (1998). J. Biol. Chem. 273, 33759-33765

Ward DG & Cavieres JD (2003). J. Biol. Chem. 278, 14688-14697

Supported by research grants from The Wellcome Trust.

*Where applicable, the experiments described here conform with Physiological Society ethical requirements.*

## PC32

### Development of a novel method for the simultaneous measurement of free and conjugated bile acids in human serum from pregnant women with obstetric cholestasis

A.T. Dann<sup>1</sup>, K.P. Anna<sup>1</sup>, P.T. Seed<sup>1</sup>, L. Poston<sup>1</sup>, A.I. Mallet<sup>2</sup>, A.H. Shennan<sup>1</sup> and R.M. Tribe<sup>1</sup>

<sup>1</sup>Maternal and Fetal research unit, Department of Reproductive Health, Endocrinology and Development, King's College London, London, UK and <sup>2</sup>School of Science, Greenwich University, Chatham, Kent, UK

Assessment of serum bile acids is central to the diagnosis of many liver disorders. The methods currently available are time consuming and do not allow the simultaneous measurement of a range of bile acids and their associated conjugates. The aim of this study was to develop a high performance liquid chromatography (HPLC) electrospray ionisation mass spectrometry (MS) technique to investigate bile acid metabolism in human serum from normal pregnant women and pregnant women with the liver disorder obstetric cholestasis (OC).

Bile acids profiles were investigated in fasted serum from pregnant women with OC (n=41) and normal healthy pregnant women (controls, n = 11) in the third trimester 37.6±1.3 and 39.9 ±1.4 weeks' ± SD respectively. Informed consent was obtained. Comparisons were made using linear regression with robust standard errors and geometric means with 95% confidence intervals (CI).

A HPLC-MS technique was validated for the simultaneous evaluation of low and high abundance conjugated and unconjugated bile acids in human serum incorporating efficient resolution, high sensitivity, good reproducibility and a low detection limit (50pg). Total bile acids were found to be significantly elevated in the OC group (Table 1), however, more relevant information was gained by investigating the differential bile acid profile and state of conjugation. Table 1 details the most abundant bile acids in serum. We demonstrated that bile acids are predominately conjugated with glycine and taurine in the maternal circulation. In OC taurine conjugates predominate and primary bile acids account for the majority of the increases in serum bile acid concentrations.

This method has been used to measure abnormal bile acid profiles in women with OC and will potentially be a useful tool for the assessment of serum bile acid profiles in other liver diseases. An improved evaluation of bile acid metabolism may provide better diagnostic or pathophysiological information in liver disease.

**Table 1. Bile acid (BA) biochemistry.**

	OC n=41 Mean(95% CI)	Control n=11 Mean(95% CI)	Comparison P value
Total BA (enzymatic method) $\mu\text{mol/L}$	12.6 (9.8-15.2)	6 (4.4-9.2)	P < 0.001
Sum BA $\mu\text{mol/L}^*$	12.7 (10.1-16.0)	4.6 (2.7-7.7)	P < 0.001
Taurocholic acid $\mu\text{mol/L}^*$	4.6 (3.4-6.4)	0.4 (0.2-0.9)	P < 0.001
Taurochenodeoxycholic acid $\mu\text{mol/L}^*$	1.7 (1.3-2.4)	0.5 (0.2-1.3)	P = 0.006
Tauroodeoxycholic acid $\mu\text{mol/L}^*$	0.2 (0.1-0.4)	0.3 (0.1-0.8)	P = 0.335
Glycocholic acid $\mu\text{mol/L}^*$	2.4 (1.8-3.2)	0.6 (0.3-1.1)	P < 0.001
Glycochenodeoxycholic acid $\mu\text{mol/L}^*$	1.1 (0.9-1.4)	0.7 (0.3-1.3)	P = 0.134
Glycodeoxycholic acid $\mu\text{mol/L}^*$	0.1 (0.1-0.3)	0.4 (0.2-0.7)	P = 0.100

measured by HPLC-MS

This work was supported by Tommys', the Baby Charity [No: 1060508], Lauren Page Trust and University of London Triangle Trust.

Where applicable, the experiments described here conform with Physiological Society ethical requirements.

## PC33

### Histamine-mediated smooth muscle contraction in isolated chicken small intestine occurs via selective $\text{Ca}^{2+}$ channel activation

C.B. Collins, T. Quinn, A.W. Baird and D.P. Campion

Department of Veterinary Physiology and Biochemistry, Conway Institute of Biomolecular & Biomedical Sciences, University College Dublin, N.U.I., Dublin 4, Ireland

Histamine, a primary mediator of the inflammatory response, is a potent spasmogen of smooth muscle. Sources of activator  $\text{Ca}^{2+}$  for histamine-induced contraction of avian intestinal smooth muscle have not been described. The aim of this study was to assess the contribution of intracellular and extracellular  $\text{Ca}^{2+}$  to histamine-mediated contractions.

Male Cobb 500 chickens (aged 21-42 days) were humanely killed using  $\text{CO}_2$  asphyxiation. Full thickness longitudinal intestinal smooth muscle strips were suspended under 1 g of tension, in a physiological buffer at 37°C gassed with 95%  $\text{O}_2$  /5%  $\text{CO}_2$ . Isometrically measured contractile responses were expressed as a % of the response to carbachol (CCh, 100 $\mu\text{M}$ ). Statistical analyses were made using Student's unpaired two-tailed t-test or analysis of variance.

Cumulative addition of histamine (0.01-100  $\mu\text{M}$ ) caused rapid onset, concentration-dependent, sustained contractions of muscle strips ( $\log \text{EC}_{50} = -5.4 \pm 0.2$ ) with the peak tissue responses reaching  $76 \pm 9\%$  of the maximum CCh response (mean  $\pm$  SEM, n = 28). The histamine concentration-response curve was sensitive to mepyramine (1  $\mu\text{M}$ ) but not cimetidine (1  $\mu\text{M}$ ) nor thioperamide (1  $\mu\text{M}$ ), indicating that histamine primarily acts via H1 receptors.

Histamine-induced contractions were abolished in a nominally  $\text{Ca}^{2+}$ -free medium containing 1mM EDTA (p<0.005, n=5). Pre-treatment with the L-type voltage-operated  $\text{Ca}^{2+}$  channel blocker nifedipine (1 $\mu\text{M}$ ) caused a significant reduction in basal tone (p<0.05, n=5) but had no effect on histamine-induced contractions. Pre-incubation with SK&F 96365 (50 $\mu\text{M}$ ), a blocker of both

receptor-activated and voltage-operated  $\text{Ca}^{2+}$  channels, significantly reduced the peak contractile response to histamine ( $25 \pm 9\%$ ,  $p(0.0005, n=6)$ ) and also reduced initial resting tension ( $p(0.05)$ ). The selective sarcoplasmic reticulum  $\text{Ca}^{2+}$  pump inhibitor thapsigargin ( $1\mu\text{M}$ ), used to deplete intracellular  $\text{Ca}^{2+}$  stores, had no effect on basal tone or on histamine-mediated contractions ( $n=5$ ). In conclusion it would appear that histamine-induced contractions of chicken small intestine smooth muscle are heavily dependent on extracellular  $\text{Ca}^{2+}$  influx via receptor-activated  $\text{Ca}^{2+}$  channels. Intracellular  $\text{Ca}^{2+}$  release appears to have little role to play in histamine-mediated contractions. The basal tone of the tissue is both SK&F 96365 and nifedipine sensitive, suggesting that different  $\text{Ca}^{2+}$  channels may contribute to the maintenance of resting tone and histamine-mediated contractions.

This work was supported by the Higher Education Authority of Ireland.

*Where applicable, the experiments described here conform with Physiological Society ethical requirements.*

#### PC34

##### **Modulation of murine hepatic portal vein rhythmicity by food intake**

I. Greenwood, M. Roe, L. Patterson, M. Skasick and P. Andrews  
*Basic Medical Sciences, St George's Hospital Medical School, London, UK*

The hepatic portal vein (HPV) is a rhythmically active blood vessel situated between the gastrointestinal tract and the liver that supplies 80% of the blood perfusing the liver. Whilst the generation of spontaneous activity by PVs from different species is well documented there is no information on the regulation of this activity by dietary factors. The present study investigated whether there was any influence of food intake on the spontaneous activity of HPV from adult balb-C mice. HPVs were harvested from fed animals or mice deprived of food for 16 h (fasted) and humanely killed. HPVs were mounted for isometric tension recording in standard tissue baths containing Krebs solution at  $37^\circ\text{C}$  and aerated with 95% $\text{O}_2$ /5% $\text{CO}_2$ . All tissues studied were spontaneously active within 10 mins of mounting. In HPVs from fed animals the activity exhibited a number of different contractile patterns ranging from single contractions to bursts of contractions whereas in all HPVs from fasted animals only single contractions were recorded. The mean interval between contractions was significantly longer in HPVs from fed animals ( $6.3 \pm 0.2$  s compared to  $4.7 \pm 0.12$  s, mean  $\pm$  SEM,  $p < 0.001$ , data from 25 and 14 animals respectively). The duration of individual contractions was also briefer in HPVs from fasted mice ( $4.2 \pm 0.09$  s v  $5.74 \pm 0.22$  s,  $p < 0.001$ , Student's *t* test) and individual contractions were significantly smaller ( $0.1 \pm 0.02$  g compared to  $0.18 \pm 0.01$  g,  $p < 0.01$ ). In comparison the effects of exogenously applied phenylephrine and 5-HT ( $100\mu\text{M}$ ) were not significantly different between both groups. However the maximal response to 60 mM KCl was smaller in HPVs from fasted mice ( $0.17 \pm 0.02$  g compared to  $0.21 \pm 0.02$  g,  $p < 0.05$ ,  $n=9$  and 14). These data show that food deprivation has a profound effect on PV rhythmicity.

IAGs work is sponsored by the British Heart Foundation and BBSRC.

*Where applicable, the experiments described here conform with Physiological Society ethical requirements.*

#### PC35

##### **Expression of KCC3 protein in gastric parietal cells**

T. Fujii<sup>1</sup>, Y. Takahashi<sup>1</sup>, Y. Itomi<sup>1</sup>, M. Morii<sup>1</sup>, N. Horikawa<sup>2</sup>, K. Tsukada<sup>2</sup>, N. Takeguchi<sup>1</sup> and H. Sakai<sup>1</sup>

<sup>1</sup>*Department of Pharmaceutical Physiology, Toyama Medical and Pharmaceutical University, Toyama city, Japan and* <sup>2</sup>*Department of Surgery II, Toyama Medical and Pharmaceutical University, Toyama city, Japan*

The  $\text{K}^+$ - $\text{Cl}^-$  cotransporter (KCC) plays a significant role in the cell volume regulation, epithelial transport and ion homeostasis of many cell types (Hebert *et al.* 2004). So far, four KCC isoforms (KCC1-4) have been cloned. KCC1 and KCC4 are expressed ubiquitously. KCC2 is expressed in neurons in the central nervous system and retina. KCC3 is abundant in muscle, brain, spinal cord, kidney, heart, pancreas and placenta. So far, the expression of KCC isoforms in stomach has not been reported.

Here we tested whether KCC isoforms are expressed in rat, mouse, rabbit and human gastric mucosa. Rats and mice were humanely killed by cervical dislocation. Rabbits were humanely killed by the intraperitoneal administration of an overdose of urethane ( $2\text{ g kg}^{-1}$ ). Isolated rabbit gastric glands were prepared as previously described (Sakai *et al.* 2003). Human gastric specimens were obtained from surgical resection of Japanese patients with gastric cancer in accordance with the recommendations of the Declaration of Helsinki and with the ethics committee approval. The expression of KCC mRNA and the protein in the samples was examined by Northern blotting and Western blotting, respectively. The distribution of KCC protein in the tissue sections was examined by immunohistochemistry.

Using isolated gastric mucosa and the gastric parietal cells of rats and rabbits, we compared the expression level of KCC1, 3, and 4 mRNAs between the mucosa and the parietal cells. Northern blot analysis showed that only KCC3 mRNA is more abundant in the parietal cells compared with the gastric mucosa. In rats, the expression level of KCC3 mRNA in the parietal cells was ( $4.7 \pm 0.2$ )-fold higher than that in the gastric mucosa ( $n = 3$ ,  $P < 0.01$ ). In rabbits, the expression level of KCC3 mRNA in the gastric parietal cells was ( $2.0 \pm 0.2$ )-fold higher than that in the gastric mucosa ( $n = 3$ ,  $P < 0.05$ ). Western blot analysis using a specific anti-KCC3 antibody showed the expression of KCC3 protein ( $\sim 160$  and  $\sim 190$  kDa) in isolated gastric mucosa of rats, mice and humans, and in isolated rabbits gastric glands ( $n = 3-5$ ). Immunohistochemistry in isolated mucosa of rats, mice and rabbits showed the expression of KCC3 protein in the parietal cells ( $n = 3-5$ ). In human gastric cancer tissue, decreased expression of the KCC3 protein was observed ( $n = 3$ ).

These results suggest that KCC3 is abundantly expressed in the gastric parietal cells and it may be involved in the mechanism of gastric acid secretion.

Hebert SC *et al.* (2004). *Pflügers Arch.* 47, 580-593.

Sakai H *et al.* (2003). *J. Physiol.* 551, 207-217.

*Where applicable, the experiments described here conform with Physiological Society ethical requirements.*